

# Coding of Time-Varying Electric Field Amplitude Modulations in a Wave-Type Electric Fish

RALF WESSEL, CHRISTOF KOCH, AND FABRIZIO GABBIANI

*Neurobiology Unit, Scripps Institution of Oceanography, University of California at San Diego, La Jolla 92093-0202; and Computation and Neural Systems Program, 139-74 California Institute of Technology, Pasadena, California 91125*

## SUMMARY AND CONCLUSIONS

1. The coding of time-varying electric fields in the weakly electric fish, *Eigenmannia*, was investigated in a quantitative manner. The activity of single P-type electroreceptor afferents was recorded while the amplitude of an externally applied sinusoidal electric field was stochastically modulated. The amplitude modulation waveform (i.e., the stimulus) was reconstructed from the spike trains by mean square estimation.

2. From the stimulus and the reconstructions we calculated the following: 1) the signal-to-noise ratio and thus an effective temporal bandwidth of the units; 2) the coding fraction, i.e., a measure of the fraction of the time-varying stimulus encoded in single spike trains; and 3) the mutual information provided by the reconstructions about the stimulus.

3. Signal-to-noise ratios as high as 7:1 were observed and the bandwidth ranged from 0 up to 200 Hz, consistent with the limit imposed by the sampling theorem. Reducing the cutoff frequency of the stimulus increased the signal-to-noise ratio at low frequencies, indicating a nonlinearity in the receptors' response.

4. The coding fraction and the rate of mutual information transmission increased in parallel with the standard deviation (i.e., the contrast) of the stimulus as well as the mean firing rate of the units. Significant encoding occurred 20–40 Hz above the spontaneous discharge of a unit.

5. When the temporal cutoff frequency of the stimulus was increased between 80 and 400 Hz, 1) the coding fraction decreased, 2) the rate of mutual information transmission remained constant over the same frequency range, and 3) the reconstructed filter changed. This is in agreement with predictions obtained in a simplified neuronal model.

6. Our results suggest that 1) the information transmitted by single spike trains of primary electrosensory afferents to higher-order neurons in the fish brain depends on the contrast and the cutoff frequency of the stimulus as well as on the mean firing rate of the units; and 2) under optimal conditions, more than half of the information about a Gaussian stimulus that can in principle be encoded is carried in single spike trains of P-type afferents at rates up to 200 bits per second.

## INTRODUCTION

The electric fish, *Eigenmannia*, generates quasisinusoidal electric organ discharges (EODs) at individually fixed frequencies (250–600 Hz) for electrolocation and communication (for reviews, see Bullock and Heiligenberg 1986; Heiligenberg 1991). The fish detect objects in the environment by sensing local perturbations in the phase and the amplitude of the electric field with tuberous electroreceptors located on the body surface (Bastian 1986; Zakon 1986). For at least one specific behavior, the jamming avoidance response,

these two features of the electric field are combined in order to compute whether the EOD frequency should be raised or lowered by the animal (Heiligenberg and Partridge 1981). Although it is known that phase information is processed with a remarkable temporal resolution by the electrosensory system (Kawasaki et al. 1988; Rose and Heiligenberg 1985), the coding of time-varying amplitude modulations has not yet been investigated in detail. We characterize here in a rigorous manner the ability of single afferents to represent temporal electric field amplitude modulations.

The tuberous receptor cells in an electroreceptor organ are innervated by boutons from single afferent axons projecting to the electrosensory lateral line lobe of the medulla. The number of receptor organs contacted per afferent axon forms a bimodal distribution in adult *Eigenmannia* (Zakon 1987; see also Sanchez and Zakon 1990), thus allowing for two types of tuberous receptors: time coders (T-type) and amplitude coders (P-type). Tuberous receptors are tuned to the EOD frequency of the individual. They respond to a low-amplitude sinusoidal electric field at their best frequency by firing in a loosely phase-locked manner, with a probability of firing  $<1$  per electric field cycle. As the amplitude of the electric field is increased, the probability of firing increases, and for a sufficiently large amplitude, electroreceptor afferents phase-lock 1:1 and fire once for each cycle of the sinusoidal electric field. The tuning curves, i.e., the isothreshold curves for 1:1 phase-locking taken over a range of stimulus frequencies, are V-shaped, T receptors being more sensitive and more sharply tuned than P receptors (Hopkins 1976). In the physiological range of frequency and amplitude of the electric field, T-type electroreceptor afferents fire in a phase-locked manner once for each cycle of the electric field, whereas P-type electroreceptor afferents fire in a loosely phase-locked manner with a probability of  $<1$  per cycle (Bastian and Heiligenberg 1980; Scheich et al. 1973; but see also Viancour 1979).

In this study, the coding of amplitude-modulated electric fields in spike trains of P-type units was investigated. Measures of coding such as the signal-to-noise ratio, the coding fraction, and the rate of mutual information transmission were calculated. The spike trains and the white noise amplitude modulations were analyzed with the use of mean square stochastic estimation (Poor 1994; Saleh 1978; Wiener 1949). This allows us to compute a filter that, when convolved with the spike train of the neuron in response to the time-varying stimulus, produces an optimal reconstruction of the stimulus (Bialek et al. 1991; Rieke et al. 1993; see

also Theunissen et al. 1996; Warland and Meister 1993). This method was applied 1) to study the coding of amplitude modulations at the input stage of the electrosensory system of electric fish, and, more generally, 2) to explore how the measures of coding depend on the statistics of the stimulus, the spontaneous activity and the mean firing rate of neurons.

## METHODS

### Stimulus and electrophysiology

Adult specimens of *Eigenmannia*, 15–20 cm long, were acquired from tropical fish dealers under the commercial name glass knife fish and maintained at 25°C in aquarium water adjusted for resistivity to a value of 10–20 kΩ/cm and having a pH of 7. Before an experiment, the fish's EOD frequency was measured. The animal was then injected intramuscularly with 20 μl (2 mg/ml) of Flaxedil (gallamine triethiodide, Sigma, St Louis, MO) to paralyze the fish and to block the myogenic EOD. Experiments were performed in water of 8–10 kΩ/cm resistivity, a pH of 7, and a temperature of 25°C. The fish was gently held on its side by a foam-lined clamp and ventilation was provided by a stream of aerated water led into the animal's mouth through a glass tube. A residual EOD-related signal could be detected with a pair of wire electrodes placed next to the tail. To record the activity of single afferent units from electroreceptor organs located on the animal's trunk, the posterior branch of the anterior lateral line nerve was exposed just rostral to the operculum. Recordings were made with the use of 1 M KCl-filled glass electrodes (40–60 MΩ) and an amplifier (WPI M707A, Sarasota, FL). The indifferent electrode was a silver wire placed around the recording electrode like a small ring.

The electric field in the water was established by a pair of chlorided silver electrodes, one placed in the mouth and one near the tail of the fish (positive pole at the mouth; see Fig. 1A). The stimulus voltage was generated by a function generator (Exact 519, Hillsboro, OR) coupled to the electrodes by a transformer. The voltage generating the electric stimulus,  $V(t)$ , had a mean amplitude,  $A_0$  and a carrier frequency,  $f_{\text{carrier}}$ , and was modulated according to

$$V(t) = A_0[1 + s(t)] \cos(2\pi f_{\text{carrier}} t) \quad (1)$$

The carrier frequency was set to the value of the fish's electric EOD frequency before curarization (typically slightly larger than 400 Hz for the fish selected in these experiments), and  $s(t)$  was a random, zero-mean voltage having a flat (white) power spectrum up to a variable cutoff frequency,  $f_c$ , and a variable standard deviation,  $\sigma$ . The function generator is designed so that a value  $s(t) = +1$  V doubles the amplitude, whereas  $s(t) = -1$  V reduces the amplitude to 0. The white noise,  $s(t)$ , was produced by playing a blank tape on a tape recorder (HP3964A, Loveland, CO). This signal was then filtered through a flat-amplitude low-pass filter (2 4-pole Butterworth filters in series, Wavetek Rockland 452, San Diego, CA), and attenuated with a voltage divider before being fed into the external amplitude-modulated input of the function generator. This allowed us to vary  $f_c$  and the standard deviation of the stimulus (see Fig. 1C and *Theory*, below;  $\sigma^2$  is equal to the integrated power spectral density of the stimulus). An increase in  $f_c$  is reflected in the time domain by a decrease in the autocorrelation width of the stimulus (see Fig. 1C, *inset*). This occurs because variations in the stimulus take place on a faster time scale when higher frequencies are included. The electric field was monitored with bipolar electrodes placed close to the side fin and oriented perpendicularly to the skin. Mean amplitudes at the side fin,  $A_{\text{sf}}$ , were typically in the physiological range of the order of 1 mV/cm (see RESULTS). Because the location of the receptors was not

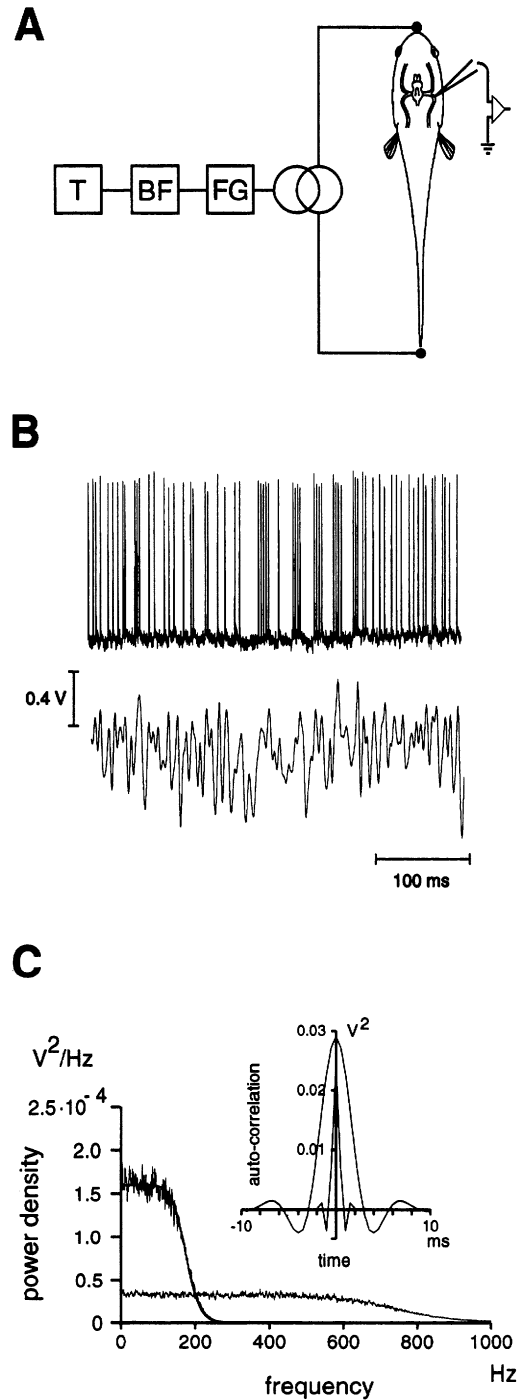


FIG. 1. A: schematic drawing of the experimental setup. A blank tape was played on a tape recorder (T), and the output signal was passed through a low-pass filter with variable cutoff frequency (BF) before being fed into the function generator (FG). The electric field was generated by 2 electrodes placed in the mouth and near the tail of the fish. The stimulus isolation unit is represented by the 2 intersecting circles. B: typical example of an extracellular spike train and sample stimulus. The cutoff frequency of the stimulus was 175 Hz, and its power spectrum is shown in C. C: power spectra of 2 different stimuli with  $f_c$ s of 175 and 740 Hz. The thick line superposed to the largest power spectral density ( $f_c = 175$  Hz) is the best fit obtained from the transfer function of the low-pass Butterworth filter. The 2 stimuli had a standard deviation  $\sigma$  of 0.16 V (wide band,  $f_c = 740$  Hz) and 0.17 V (short band,  $f_c = 175$  Hz). *Inset*: autocorrelation function of the 2 signals. The width of autocorrelation (that is, the time interval of significant correlation in 2 stimulus values) decreases with increasing  $f_c$ .

mapped in these experiments and the electric field was inhomogeneous, the value of the mean amplitude of the electric field at the location of the receptors was not known. The afferent recordings together with the white noise (see Fig. 1B) were stored on magnetic tape (sampling rate 20 kHz, Vetter Instruments 3000A, Rebersburg, PA) and later A-D converted (sampling rate 10 kHz, Datapac II, Run Technologies, Laguna Hills, CA).

Electroreceptor afferents were identified as P-type and included in this study when 1) the probability of firing per period of the EOD was  $< 1$  in the physiological range of the electric field amplitude; 2) the spontaneous activity was irregular (P-type), as opposed to bursting (T-type) (Scheich et al. 1973); and 3) the units phase-locked with large jitter (P-type) as opposed to small jitter (T-type) (Bastian and Heiligenberg 1980; Scheich et al. 1973). Thus 26 units were selected for further analysis. Once a unit was selected, the following protocols, each having a duration of 135 s, were performed as time permitted. 1) The spontaneous activity was measured. 2) The response to wide-band ( $f_c = 740$  Hz) white noise was recorded. 3) The values of  $f_c$ , the mean amplitude,  $A_o$ , and the standard deviation,  $\sigma$ , of the white noise,  $s(t)$ , were changed in a pseudorandom manner. The range of values used for the standard deviation,  $\sigma$ , was limited to  $\sigma < 0.25$  V (i.e., mean variations of at most 25% in the amplitude of the electric field) in order to ensure that  $A(t) = A_o [1 + s(t)] \geq 0$ . Negative values of  $A(t)$  would have introduced phase changes in addition to amplitude changes in the signal given by Eq. 1. When the mean amplitude,  $A_o$ , was changed, values covered typically a range of 20 dB around the mean value of  $A_o$ .

### Theory

The data were analyzed with the use of the following algorithm (Bialek et al. 1991; Gabbiani 1996; Gabbiani and Koch 1996). Let

$$x(t) = \sum_i \delta(t - t_i) - x_o \quad (2)$$

be the spike train (where  $t_i$  are the spike occurrence times) recorded in response to the stimulus, with the mean firing rate,  $x_o$ , subtracted. A linear estimate,  $s_{\text{est}}(t)$ , of the stimulus,  $s(t)$ , given the spike train, was obtained by convolving  $x(t)$  with a filter,  $h(t)$

$$s_{\text{est}}(t) = \int_0^T dt' h(t - t') x(t') \quad (3)$$

The filter,  $h(t)$ , is to be chosen in such a way as to minimize the mean square error,  $\epsilon^2$ , between the stimulus and estimate

$$\epsilon^2 = \frac{1}{T} \int_0^T dt [s(t) - s_{\text{est}}(t)]^2 \quad (4)$$

where the integration is over the duration ( $T = 135$  s) of the experiment. An explicit formula (Poor 1994; Wiener 1949) for this filter is

$$h(t) = \int_{-f_c}^{f_c} df \frac{S_{sx}(-f)}{S_{xx}(f)} e^{-i2\pi ft} \quad (5)$$

where  $f_c$  is the cutoff frequency of the stimulus and  $S_{sx}(f)$  and  $S_{xx}(f)$  are the Fourier transforms of the cross-correlation and the autocorrelation functions of the stimulus and spike trains

$$R_{sx}(\tau) = \frac{1}{T} \int_0^T dt s(t)x(t + \tau) \quad \text{and} \quad R_{xx}(\tau) = \frac{1}{T} \int_0^T dt x(t)x(t + \tau)$$

respectively. The filter given in Eq. 5 will not be causal in general [i.e.,  $h(t) \neq 0$  for  $t > 0$ , see RESULTS]. Causality is usually implemented by introducing a delay in the reconstructions (Bialek et al. 1991) or by the use of a causal Wiener-Kolmogorov filter (Poor

1994). Once the best linear estimate,  $s_{\text{est}}(t)$ , is determined, the “noise” contaminating the reconstructions is defined as

$$n(t) = s_{\text{est}}(t) - s(t)$$

Let  $S_{nn}(f)$  be the power spectrum of the noise and  $S_{ss}(f)$  the power spectrum of the stimulus. The signal-to-noise ratio is defined as

$$\text{SNR}(f) = \frac{S_{ss}(f)}{S_{nn}(f)} \quad (6)$$

and is a measure of the amount of signal power present at a given frequency relative to the noise contaminating the reconstructions.

In the extreme case where the spike train is completely unrelated to the signal,  $\text{SNR}(f) = 1$  for all frequencies,  $f$ , otherwise  $\text{SNR}(f) > 1$ . It can be shown (Gabbiani and Koch 1996) that the mean square error in the reconstructions is

$$\epsilon^2 = \int_{-f_c}^{f_c} df \frac{S_{ss}(f)}{\text{SNR}(f)}$$

and takes its maximal value,  $\epsilon^2 = \sigma^2$ , when  $\text{SNR}(f) = 1$  for all frequencies  $f$ . Thus the coding fraction,  $\gamma$ , defined as

$$\gamma = 1 - \frac{\epsilon}{\sigma}$$

is a normalized measure of the quality of reconstructions, taking values between 0 (when the reconstructions are not better than chance) and 1 (when 100% of the stimulus standard deviation has been reconstructed, that is, the reconstructions are perfect). The coding fraction can thus be compared across experiments.

For a Gaussian white noise stimulus, the  $\epsilon$ -entropy or rate distortion function, defined as

$$I_\epsilon = \frac{-f_c}{\log(2)} \log\left(\frac{\epsilon}{\sigma}\right) \quad (\text{in bits/s}) \quad (7)$$

is a measure of the rate of mutual information transmitted by the reconstructions about the stimulus (see Gabbiani 1996; Kolmogorov 1956; Shannon 1963, sect. 27 and 28). Dividing by the mean firing rate,  $\lambda$ , of the unit yields the mutual information transmitted per spike,  $I_s = I_\epsilon/\lambda$ .

### Data analysis

The spike peak occurrence times were selected and resampled at 2 kHz together with the stimulus,  $s(t)$ . This precision was sufficient because only frequencies well below the Nyquist frequency of the digitization (1,000 Hz) were of interest (see RESULTS). Estimates of the stimulus and spike train power spectra were obtained with the use of a fast Fourier algorithm and Bartlett windowing (see Press et al. 1992), and by averaging 130 samples of data (1,024 ms long). The same analysis was performed to obtain estimates of the cross-correlation between spike trains and stimuli and, later on, the power spectrum of the noise in the reconstructions. Because the total recording time used to compute these estimates was 135 s and P units had typical firing rates  $> 100$  Hz in these experiments,  $> 10,000$  spikes were averaged. The cutoff frequency of the stimulus was estimated by fitting the squared gain of the low-pass filter transfer function (2 4-pole Butterworth filters in series; Oppenheim and Schaffer 1989) to the power spectrum of the stimulus,  $s(t)$  (see the 2 superposed traces for the lower  $f_c$  in Fig. 1C). The optimal linear filter,  $h(t)$ , was obtained by deconvolving the cross-correlation of the spike train and stimulus with the power spectrum of the spike train according to Eq. 5 (see Theory, above). The reconstructions were obtained by computing the convolution of the filter and spike train,  $x(t)$ , (see Eqs. 2 and 3) in the frequency domain with the use of a fast Fourier transform. To avoid contamination by the carrier frequency of the spike train (see RESULTS and

Fig. 2, *C2* and *C3*), all the numerical Fourier components of the filter were set to 0 for frequencies greater than  $f_{\text{carrier}} - 30$  Hz. Because  $f_{\text{carrier}}$  was typically  $>400$  Hz for the fish selected in these experiments and signal-to-noise ratios were always equal to 1 for frequencies  $>200$  Hz (see RESULTS and Fig. 3*A1*), these frequency components can be safely neglected. The integration over time, giving the mean square error in Eq. 4, was calculated with the use of the trapezoidal rule. Experimental errors were either obtained directly by repeated measurements (standard deviation over 10 different trials of the same experiment) or by error propagation (Bronshstein and Semendyayev 1985, sect. 2.1.2).

The reconstructions described above were also compared (see *Mean firing rate*, below, and Fig. 2*D*) with reconstructions obtained by the use of the cross-correlation between the stimulus and spike train divided by the mean firing rate of the units,  $R_{\text{sx}}(t)/\lambda$ , in place of the optimal filter,  $h(t)$ , in Eq. 3. The cross-correlation function  $R_{\text{sx}}(\tau)$  (also called reverse correlation when  $\tau > 0$ , see *Theory*, above) is proportional to the mean stimulus preceding and following a spike. It is thus plausible that an estimate of the stimulus could be obtained by convolving the spike train with  $R_{\text{sx}}(t)$  (Gielen et al. 1988). However, such reconstructions will not satisfy an optimality principle (such as minimizing the mean square error). Furthermore, the dimensional units of the cross-correlation ( $V \cdot \text{spikes} \cdot \text{s}^{-1}$  in the present case) do not coincide with the units required for a reconstruction filter ( $V$ ). It has been shown (Gabbiani and Koch 1996) that dividing  $R_{\text{sx}}(t)$  by the mean firing rate yields a reconstruction filter with correct dimension that converges to the optimal filter  $h(t)$  for idealized neuron models in the limit of low firing rate.

## RESULTS

### *Response to sinusoidal and stochastic amplitude modulations—spontaneous activity*

As is well known, P receptor afferent units fire with increased probability when the amplitude of an external electric field is raised (see, for example, Scheich et al. 1973). This is illustrated in Fig. 2*A*, where the response of a P unit to a 10-Hz sinusoidal amplitude modulation and the corresponding poststimulus histogram are shown. The firing probability rose as the amplitude of the electric field increased (Fig. 2*A*, *inset*) (Bastian and Heiligenberg 1980) and the peak response showed a slight shift to the left with respect to the peak stimulus in accordance with earlier results (Heiligenberg 1986; Hopkins 1976).

The spontaneous activity was studied in 17 units. Spontaneous mean firing frequencies were widely distributed between 0 and 100 Hz, as previously observed (see Fig. 2*B1*) (Viancour 1979). The coefficient of variation of the interspike interval distributions varied from very regular (0.16) to very irregular (1.12; see Fig. 2*B2*). No systematic relationship between mean interspike interval and coefficient of variation was observed. Interspike interval distributions were usually not satisfactorily fitted by gamma distributions (Franklin and Bair 1995). In 16 of 17 units, there was a good agreement between the power spectra computed directly from the spike trains and those predicted by the interspike interval distribution under the assumption of a stationary renewal process (see Fig. 2, *B3* and *B4*) (Franklin and Bair 1995; Heiden 1969; Lukes 1961). Thus the spontaneous activity of P units appears to be consistent with the assumptions of stationarity (i.e., the statistical properties of the spike trains are independent of time) and a renewal

probability density for the spike distribution (i.e., the time of occurrence of a given spike depends on the time of occurrence of the preceding spike but not on earlier ones).

Figure 2*C1* shows the interspike interval distribution of the same P units as in Fig. 2*B3* in response to a stochastically modulated electric field ( $f_c = 88$  Hz) of increasing mean amplitude  $A_0$  (from *bottom* to *top*; see Eq. 1). The interspike interval distribution is concentrated at integral multiples of the sinusoidal carrier period,  $1/f_{\text{carrier}}$ . This translates in the Fourier domain by the appearance of peaks in the power spectrum of the spike trains at  $f_{\text{carrier}}$  and its integral harmonics (see Fig. 2*C3*). With an increase of the mean stimulus amplitude, the interspike interval distribution shifts toward intervals of shorter length (see Fig. 2*C1*, from *bottom* to *top*) and the peak power at the first harmonic increases (see Fig. 2*C2*). In other words, with increasing mean stimulus amplitude, the probability of firing increases and the unit phase-locks to the stimulus with less jitter. Similar results have been described for constant-amplitude sinusoidal stimuli (Scheich et al. 1973).

Finally, in Fig. 2*D*, the reverse correlation of the amplitude modulation with the spike train shows that spikes were typically triggered by a large positive slope in  $s(t)$ . The reverse correlation is proportional to the mean stimulus preceding a spike (De Boer and Kuyper 1968) and can therefore also be used, instead of the optimal filter  $h(t)$ , to obtain an estimate of the stimulus (see *Mean firing rate*, below).

### *Temporal bandwidth*

To estimate the effective temporal bandwidth of stimulus frequencies encoded by the units, a wide-band ( $f_c = 740$  Hz, see Fig. 1*C*) white noise stimulus was applied and the signal-to-noise ratio in the reconstructions was computed (see Eq. 6 in METHODS). A typical result is shown for one unit in Fig. 3*A1* (smallest signal-to-noise ratio); similar results were obtained for 12 additional units. Signal-to-noise ratios were always equal to 1 for frequencies  $>200$  Hz, indicating that those frequencies are not encoded. A short stretch of the corresponding stimulus and reconstructions as well as the spike train of the unit is shown in Fig. 3*A2*. Because most of the stimulus power was concentrated outside of the frequency band encoded, the quality of the reconstruction is poor;  $<2.5\%$  ( $\gamma = 0.024$ ) of the stimulus is reconstructed (Gabbiani and Koch 1996). Adjusting the cut-off frequency of the stimulus to the frequency band encoded by the units ( $f_c = 175$  Hz) while keeping its standard deviation (total power) constant (see Fig. 1*C*) improved the signal-to-noise ratio at low frequencies (see Fig. 3*A1*, largest signal-to-noise ratio) and the reconstructions reproduced the stimulus more faithfully, as shown in Fig. 3*A3* ( $\gamma = 0.222$ ).

In subsequent experiments, except during study of the effect of  $f_c$  on reconstructions (see *Cutoff frequency*, below), the  $f_c$  of the stimulus was usually set to 88 Hz, a value well within the range of frequencies encoded by the units and still covering a large portion of their optimal frequency range. This proved to be convenient because it allowed an easier study of the influence of other stimulus parameters on the quality of reconstructions.

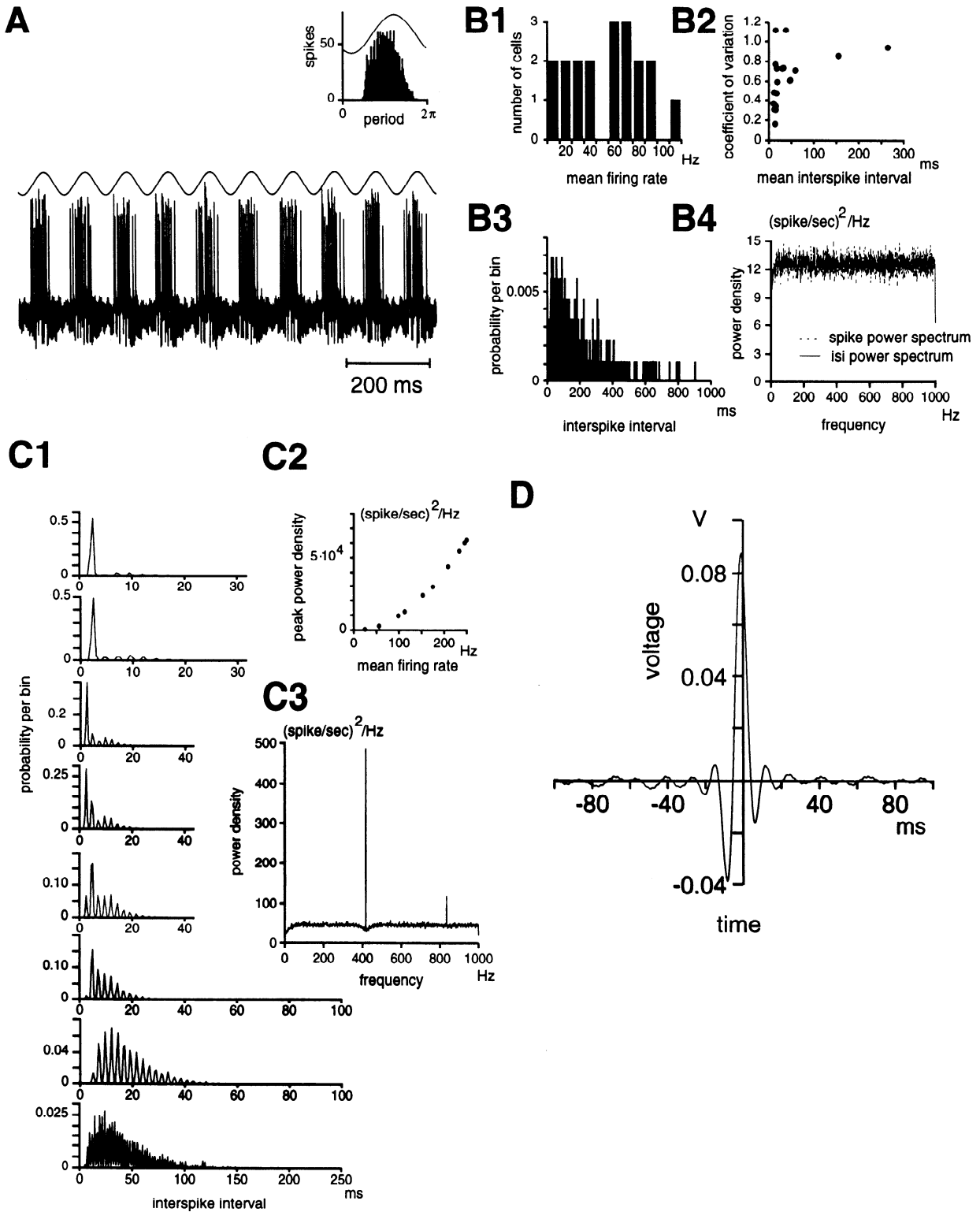


FIG. 2. *A*: response of a P receptor unit to sinusoidal amplitude modulations (10 Hz). *Inset*: poststimulus time histogram computed from 2,155 action potentials. *B1*: distribution of mean spontaneous activities in 17 units. *B2*: coefficient of variation as a function of mean interspike interval. *B3*: interspike interval distribution for 1 unit (bin size: 0.5 ms). *B4*: power spectrum of the same unit computed directly from the spike train (---) or from the interspike interval distribution (—). The prediction obtained from the interspike interval distribution is in good agreement with the actual power spectrum, as expected if the spike trains were a stationary renewal process. *C1*: from *bottom* to *top*, interspike interval distributions for increasing values of mean amplitude  $A_0$  and mean firing rate  $\lambda$  (bin size: 0.5 ms;  $\lambda = 24, 55, 98, 112, 152, 174, 208,$  and  $233$  Hz; corresponding mean amplitude at the side fin  $A_{sf} = 0.1, 0.2, 0.3, 0.4, 0.5, 0.6, 0.8,$  and  $1.0$  mV/cm). *C3*: power spectrum of the spike train at the lowest firing rate. Compared with the power spectrum in *B4*, peaks have appeared at the carrier frequency (415 Hz) and its 2nd harmonics. *C2*: peak power density at the 1st harmonics vs. mean firing rate. The stimulus had an  $f_c$  of 88 Hz. *D*: reverse correlation between spike train and stimulus for an  $f_c$  of 88 Hz divided by the mean firing rate of the cell  $[R_{sx}(t)/\lambda]$ . Similar results (a large negative-positive change in the mean stimulus preceding a spike) were also obtained at  $f_c$ s of 175 and 740 Hz.

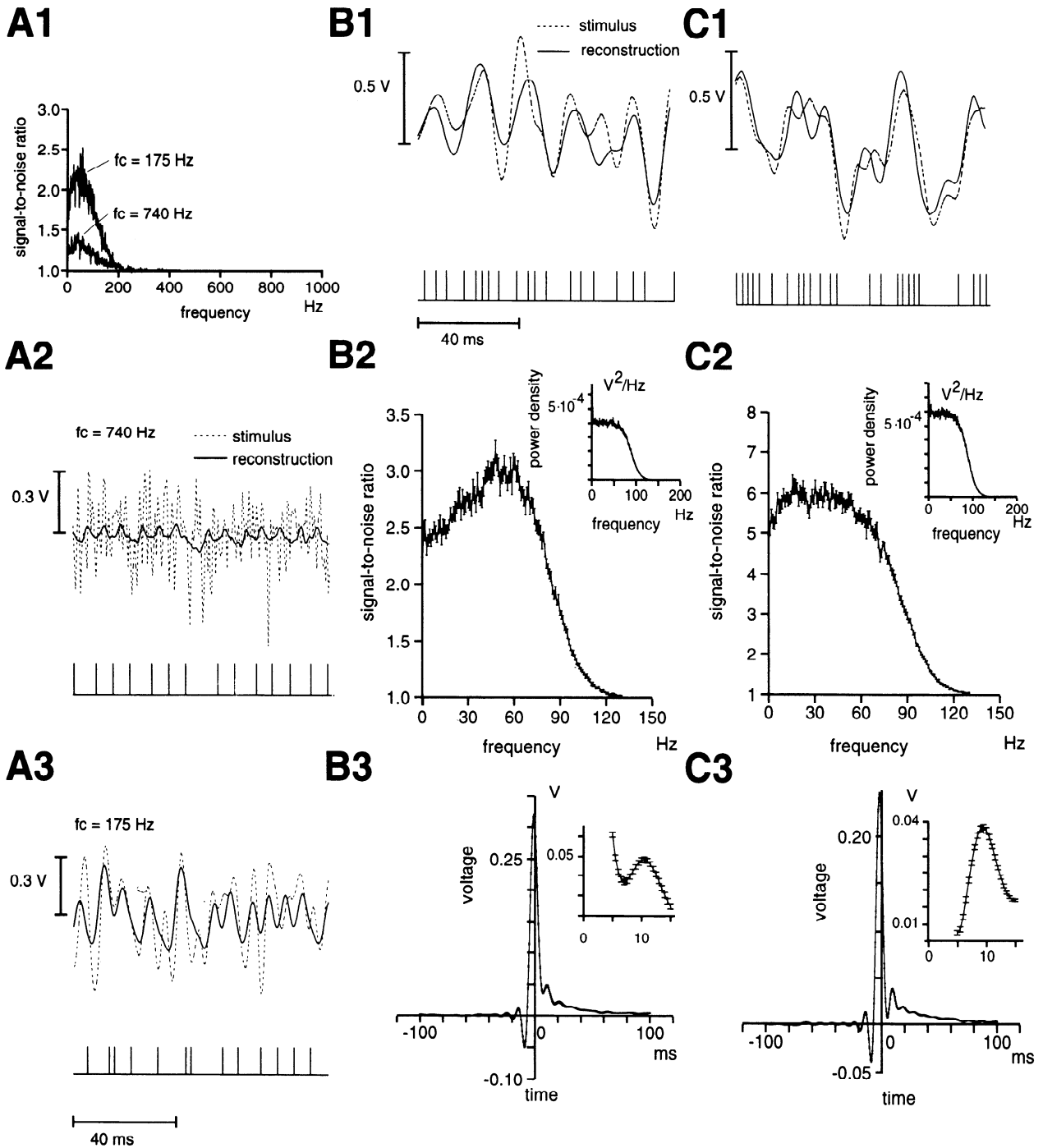


FIG. 3. *A1*: signal-to-noise ratio in response to stimuli having a high  $f_c$  (740 Hz,  $\sigma = 0.16$  V; smallest signal-to-noise ratio) and a lower  $f_c$  (175 Hz,  $\sigma = 0.17$  V; largest signal-to-noise ratio). *A2*: sample reconstructions for  $f_c = 740$  Hz (mean firing rate,  $\lambda = 139$  Hz;  $A_{sf} = 1.0$  mV/cm). *A3*: sample reconstructions for  $f_c = 175$  Hz (mean firing rate,  $\lambda = 135$  Hz;  $A_{sf} = 1.0$  mV/cm). The power spectra of the 2 stimuli were shown in Fig. 1C. *B1* and *C1*: typical stimuli ( $f_c = 88$  Hz) and reconstructions, as well as the corresponding spike trains for units *xf* and *xh*, respectively (see Table 1 for the numerical parameters and results of these experiments;  $A_{sf} = 1.0$  and 0.5 mV/cm, respectively). *B2* and *C2*: signal-to-noise ratios and power spectra of the presented stimuli (*insets*). *B3* and *C3*: reconstruction filters. *Insets* show the enlarged time course of the filters for the 1st 15 ms following a spike. The error bars are visible at this magnified scale. Although the 2 filters are similar, their detailed time course differs (compare the 2 *insets*).

*Statistics*

To study the statistical significance of our data points, we presented white noise amplitude modulations with the same parameters 10 times to a unit. Results for two units are

shown in Fig. 3, *B* (unit *xf*) and *C* (unit *xh*). Figure 3, *B1* and *C1*, shows typical traces of the stimuli, the reconstructions, and the corresponding spike trains during a trial. The next two rows show the signal-to-noise ratios, the power spectra of the presented stimuli (Fig. 3, *B2*, *C2*, and *insets*),

TABLE 1.

	$\sigma$ , V	$f_c$ , Hz	$\lambda$ , Hz	$I_c$ , bits/s	$\gamma$	$\gamma_{ub}$
Unit <i>xf</i>	$0.193 \pm 0.001$	$88 \pm 0.2$	$164 \pm 6$	$115 \pm 2$	$0.365 \pm 0.004$	0.82
Unit <i>xh</i>	$0.231 \pm 0.001$	$88 \pm 0.1$	$227 \pm 4$	$198 \pm 2$	$0.541 \pm 0.003$	0.84

Values for the standard deviation, of the stimulus ( $\sigma$ ), its cutoff frequency ( $f_c$ ), the mean firing rate ( $\lambda$ ), the rate of mutual information transmission ( $I_c$ ), and the coding fraction ( $\gamma$ ), for units *xf* and *xh* (see also Fig. 3, *B* and *C*) are means  $\pm$  SD over 10 trials. The last column reports for comparison the maximum achievable performance,  $\gamma_{ub}$ , for a rate of mutual information transmission matching the carrier frequency of the stimulus (see Eq. 8 in DISCUSSION).

and the averaged filters,  $h(t)$ , with the corresponding error bars (standard deviation over the 10 trials; Fig. 3, *B3* and *C3*). Table 1 reports the means  $\pm$  SD over the 10 experiments, for the standard deviation of the stimulus,  $\sigma$ , its  $f_c$ , the mean firing rate of the units,  $\lambda$ , the rate of mutual information transmission,  $I_c$ , and the coding fraction,  $\gamma$ . The firing rates of these two units were between 150 and 230 Hz and the portion of the stimulus reconstructed was in the range of  $1/3$ – $1/2$  of the stimulus standard deviation, corresponding to 100–200 bits per second. We conclude that in this preparation, stable recordings over a period of time of  $T = 135$  s lead to highly reproducible results and statistically significant data points.

### Cutoff frequency

The effect of the  $f_c$  of the stimulus on the coding performance was studied in 13 units and the results are summarized in Fig. 4. Although the coding fraction,  $\gamma$ , decreased with increasing  $f_c$  in all cases analyzed (see Fig. 4A; compare also Fig. 3, *A2*, *A3*, *B1*, *C1*), the mutual information rates were only weakly dependent on  $f_c$  (for  $f_c$  in the range of 80–400 Hz) in 12 of the 13 cases analyzed. A typical example is shown in Fig. 4A, *inset*. Peak rates of mutual information transmission were obtained at  $f_c = 175$  Hz ( $N = 13$ ).

The normalized reconstruction filters (peak value set to 1) of one unit computed at four different  $f_c$ s are shown in Fig. 4B3. The most significant change observed was a reduction of the filter half-width with increasing  $f_c$ . This is to be expected, because the half-width of the autocorrelation function of the signal decreases with increasing  $f_c$  (see Fig. 1C, *inset*). Thus estimation is only reliable over shorter times scales for larger  $f_c$ s. As shown in Fig. 4B2, the width at half-height of the reconstruction filter follows closely the width at half-height of the autocorrelation of the stimulus. Similar results were observed for all units studied ( $N = 13$ ). The peak values of the filter usually increased and then saturated or decreased with  $f_c$  (see Fig. 4B1).

As shown in Fig. 3A1, decreasing the  $f_c$  of the stimulus increased the signal-to-noise ratio at lower frequencies. This effect might have two different causes. 1) The power spectral density was increased in the range of frequencies encoded by the unit. 2) The power spectral density of the signal was reduced at high frequencies (compare the power spectra of the 2 stimuli in Fig. 1C). To observe in isolation these two causes, we performed two kind of experiments. 1) The  $f_c$  of the stimulus was kept fixed and the power density was increased (see *Variations in the standard deviation*, below). 2) The spectral power density of the signal was kept constant as  $f_c$  was increased. The results of this latter type of experi-

ment are shown in Fig. 4C for one unit. Increasing the frequency content of the stimulus while keeping the power density constant (see Fig. 4C, *inset*) decreased the signal-to-noise ratio at low frequencies. Similar results were found in 10 of 11 units tested. This suggests a nonlinearity in the encoding of different stimulus frequencies.

### Mean firing rate

The effect of the mean firing rate,  $\lambda$ , on the coding of time-varying amplitude modulations was studied by varying the mean amplitude  $A_0$  of the electric field (see Fig. 2C1; Scheich et al. 1973). Typical results for a single unit are shown in Fig. 5. The dynamic range of firing rates was limited at the lower end by the spontaneous activity of a unit (see Fig. 2B1) and at the upper end by  $f_{carrier}$ , because tuberous receptor afferents fire maximally one spike per carrier cycle. The signal-to-noise ratio increased with increasing mean firing rate and saturated when  $\lambda$  reached approximately half of  $f_{carrier}$  (Fig. 5, *A1* and *A2*). Similar effects were observed for the coding fraction and the rate of mutual information transmission (see Fig. 5, *B1* and *B2*). Correspondingly, the mutual information transmitted per spike reached a peak at the beginning of the saturation range and decreased for higher firing frequencies (Fig. 5B3). In 17 of 21 units analyzed, the linear filter changed with increasing mean firing rate: the integration time window of the filter shortened and a negative peak appeared at positive times. Such an example is plotted in Fig. 5C2. Peak values of the filter saturated at high firing rates and subsequently decreased in 16 of 21 cases (Fig. 5C1).

It has been shown that an estimate of the stimulus can also be obtained by convolving the spike train with the reverse correlation of the stimulus (see Fig. 2D) divided by the mean firing rate of the units (Gabbiani and Koch 1996; Gielen et al. 1988). The fraction,  $\gamma_{rev}$  (Fig. 5B1,  $\circ$ ), of the stimulus reconstructed in this way was compared with the fraction reconstructed with the use of the optimal filter (Fig. 5B1,  $\bullet$ ). As expected, the quality of reconstructions obtained with the optimal linear filter was always better than those obtained by reverse correlation, but the difference between the two reconstructions decreased with decreasing firing rate. In the worst case, reconstructions obtained by reverse correlation differed by 20% from those obtained by optimal linear reconstructions (see Fig. 5B1, *inset*). Reconstructions using reverse correlation were calculated for two additional units and similar results were observed. This shows that in these experiments, reverse correlation captures a substantial part of the time-varying stimulus, but by no mean all of it.

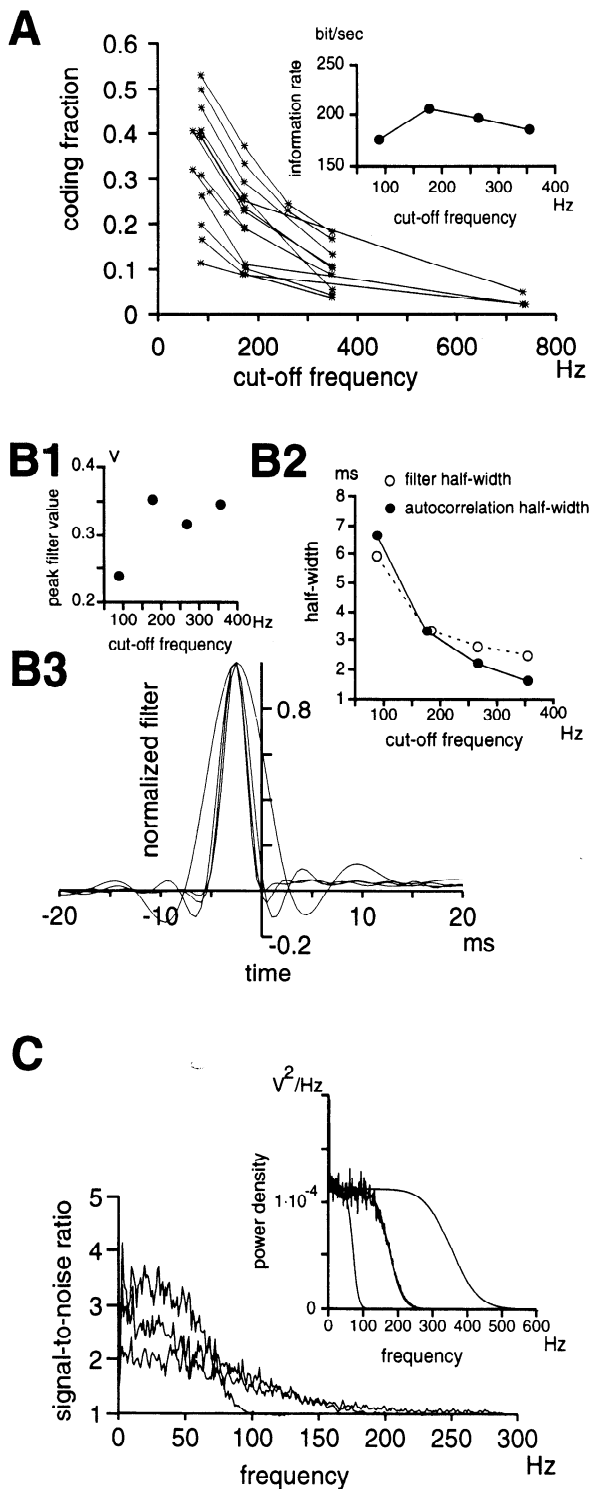


FIG. 4. A: coding fraction as a function of  $f_c$  (plotted for 13 units) and rate of mutual information transmission as a function of  $f_c$  in 1 typical example (*inset*). B3: normalized reconstruction filter for 1 unit at different  $f_c$ s (88, 175, 266, and 354 Hz). B1: peak values of the filter for these  $f_c$ s. B2: comparison of the width at half-height of the filter ( $\circ$ ) with the width at half-height of the stimulus autocorrelation function ( $\bullet$ ; see also Fig. 1C, *inset*). C: effect of adding power at high frequencies on the signal-to-noise ratio. The signal-to-noise ratio decreases (the highest signal-to-noise ratio was obtained for the lowest  $f_c$ ) as power is added at high frequencies (see *inset*; the power spectrum at the intermediate  $f_c$ , 175 Hz, was obtained directly from experimental data, whereas for the lowest and highest  $f_c$ s, 70 and 354 Hz, the fit obtained from the transfer function of the low-pass filter is shown).

Figure 6 shows the coding fraction, rate of mutual information transmission, and mutual information per spike as a function of mean firing rate for nine units that were tested with the same stimulus parameters ( $f_c = 88$  Hz,  $\sigma = 0.21$  V; experiments performed on a single unit are connected by —) and four additional units tested at a higher  $f_c$  of 175 Hz (---,  $\sigma = 0.19$  V). All units showed a very similar dependence of the coding fraction with mean firing rate:  $\gamma$  increased fairly linearly at low rates and saturated at high rates. Visual inspection of the plots suggested that the increase in coding fraction was faster for stimuli having a cutoff frequency of 88 Hz, as compared with stimuli having a higher  $f_c$  of 175 Hz. To test the significance of this hypothesis, we pooled the data from all units stimulated with  $f_c = 88$  Hz ( $N = 9$ , 60 data points), performed a linear regression, and compared the slope ( $b_1$ ) with that ( $b_2$ ) obtained for the four units stimulated at  $f_c = 175$  Hz (22 data points). Experimental points corresponding to firing frequencies  $>265$  Hz were not taken into account, because all units clearly showed saturation for firing frequencies higher than this value (see Fig. 6A). The estimated slopes and their 90% confidence intervals were disjoint [ $b_1 = 0.0024 \pm 0.0003$ , (1/Hz) and  $b_2 = 0.0017 \pm 0.0003$  (1/Hz); see Milton and Arnold 1995, chapt. 11]. Alternatively, we fitted a straight line to the coding fraction versus mean firing rate curve for each unit and performed a nonparametric comparison between the two sets of slopes thus obtained. The two populations were significantly different (Wilcoxon rank-sum test,  $\alpha < 0.01$ ; Lehmann 1975). In contrast, the increase in rates of mutual information transmission were not found to be significantly different for the two  $f_c$ s [see Fig. 6B;  $b_1 = 0.91 \pm 0.12$  (bit/Hz) and  $b_2 = 1.09 \pm 0.21$  (bit/Hz), respectively; Wilcoxon rank-sum test,  $\alpha > 0.33$ ].

Although the curves mutual information rate versus mean firing rate for one set of stimulus parameters have similar slope, they are shifted along the mean firing rate axis for different units. This shift is mainly due to the difference of spontaneous activity between units (see below) and leads to a wide distribution of the curves of mutual information per spike versus mean firing rate (Fig. 6C).

#### Spontaneous activity and stimulus coding

The spontaneous activity of the units presented in Fig. 6 ranged from 4 to 89 Hz (the lowest spontaneous activities correspond to units on the *left* of Fig. 6A, whereas units with higher spontaneous rates are shifted toward the *right*, as explained below). No significant influence of the spontaneous firing rate on the slope of the coding fraction and mutual information rate versus the mean firing rate were observed (Fig. 6, A and B). Comparing the spontaneous activity of the units with their coding fraction versus mean firing rate curves (Fig. 6A) showed that significant encoding occurred for firing frequencies 20–40 Hz above the spontaneous discharge of a unit. Correspondingly, there was a good correlation between the spontaneous activity,  $\lambda_0$ , and the intercept of the best straight line fitting each coding fraction versus mean firing rate curve (Kendall's  $\tau$  statistics and D statistics,  $\alpha < 0.01$ ) (Lehmann 1975). If the coding fraction were related to the mean firing rate by the simple linear formula  $\gamma = b_1(\lambda - \lambda_0)$ , one would expect a tight distribu-

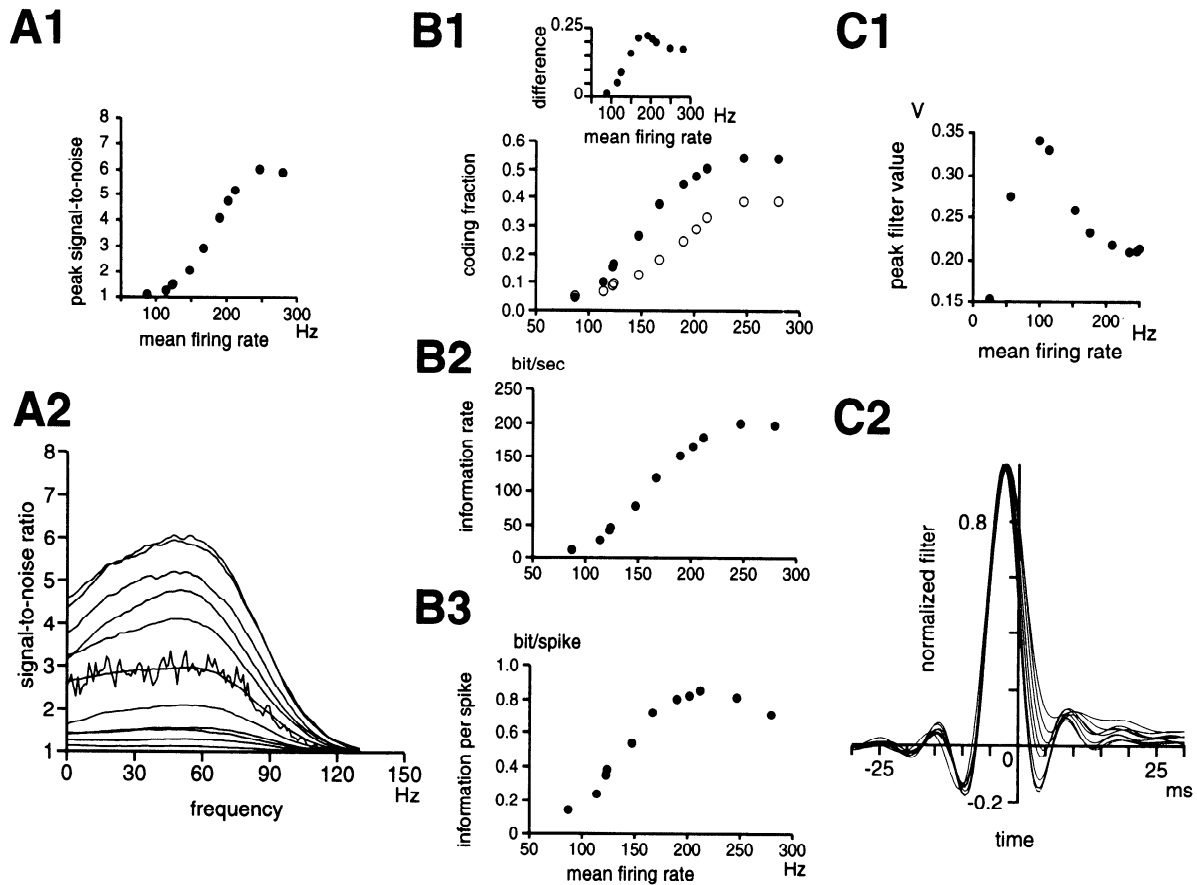


FIG. 5. Influence of mean firing rate (mean voltage amplitude  $A_0$ ) on coding for 1 unit. *A2*: signal-to-noise ratio increases as the mean firing rate increases ( $\lambda = 86, 113, 121, 123, 147, 166, 189, 201, 211, 246,$  and  $279$  Hz;  $A_{sf} = 0.4, 0.5, 0.6, 0.7, 0.8, 1.0, 1.2, 1.3, 1.4, 1.6,$  and  $2.0$  mV/cm). For better clarity, the signal-to-noise ratio has been smoothed with a Savitzky-Golay filter ( $n = 16$ ) (Press et al. 1992). A raw trace is superposed to the smoothed trace for the median value of the signal-to-noise ratio. *A1*: peak signal-to-noise ratio as a function of mean firing rate. *B1*: coding fraction for the optimal reconstructions ( $\bullet$ ) and reconstructions obtained from the reverse correlation ( $\circ$ ) as a function of the mean firing rate, the difference between the 2 is shown in the *top inset*. *B2* and *B3*: mutual information rate and mutual information transmitted per spike (computed from the *top panel*, see *Theory*). *C2*: normalized reconstruction filter for a different cell than in *A* and *B*. As the mean firing rate increases ( $\lambda = 55, 98, 112, 152, 174, 208, 233, 245,$  and  $249$  Hz;  $A_{sf} = 0.2, 0.3, 0.4, 0.5, 0.6, 0.8, 1.0,$  and  $1.4$  mV/cm), the time window of integration shortens and a negative peak appears at positive times. *C1*: peak value of the filter as a function of mean firing rate.

tion of the coding fraction versus mean firing rate curves after replotting  $\gamma$  as a function of  $\lambda - \lambda_0$  for different units. This was, however, not observed (plot not shown).

#### Variations in the standard deviation

The effect of changes in the standard deviation,  $\sigma$ , of the stimulus,  $s(t)$ , modulating the amplitude,  $A(t) = A_0[1 + s(t)]$ , of the electric field (see *Eq. 1*) were also studied. In the visual domain, this would correspond to the visual contrast. The range of values for the standard deviation was limited to  $\sigma < 0.25$  V, to avoid phase changes in the stimulus, as explained in *METHODS*. Typical results for a single unit are shown in Fig. 7. The signal-to-noise ratio increased with increasing standard deviation (Fig. 7, *A1* and *A3*). Similarly, the coding fraction, the mutual information rate, and the mutual information per spike increased with increasing standard deviation (Fig. 7, *B1–B3*). Peak values of the filter increased with standard deviation (Fig. 7*C1*), whereas the normalized filter remained largely unaltered (Fig. 7*C2*).

This last result was observed in 11 of 15 units analyzed. The mean firing rate showed some dependence on the standard deviation of the stimulus; this dependence varied from unit to unit but was usually small (Fig. 7*A2*).

Figure 8 shows the coding fraction, rate of mutual information transmission, and mutual information per spike as a function of the standard deviation for six units that were tested at the same  $f_c$ , 88 Hz. Experiments performed on a single unit are connected by a solid line. The three dashed lines correspond to one unit (*unit xr*) for which the mean firing rate was changed between experiments by changing  $A_0$  (*bottom trace*:  $\lambda = 70$  Hz, *middle trace*:  $\lambda = 110$  Hz, *top trace*:  $\lambda = 170$  Hz). For all units studied, the coding fraction, mutual information rates, and mutual information per spike increased with increasing standard deviation. The initial slope of the coding fraction versus mean firing rate curves, as well as the value of the standard deviation at which the units reached saturation, showed considerable variation. For *unit xr*, measurements taken at three different mean firing rates (Fig. 8*A*, dashed lines) showed that for

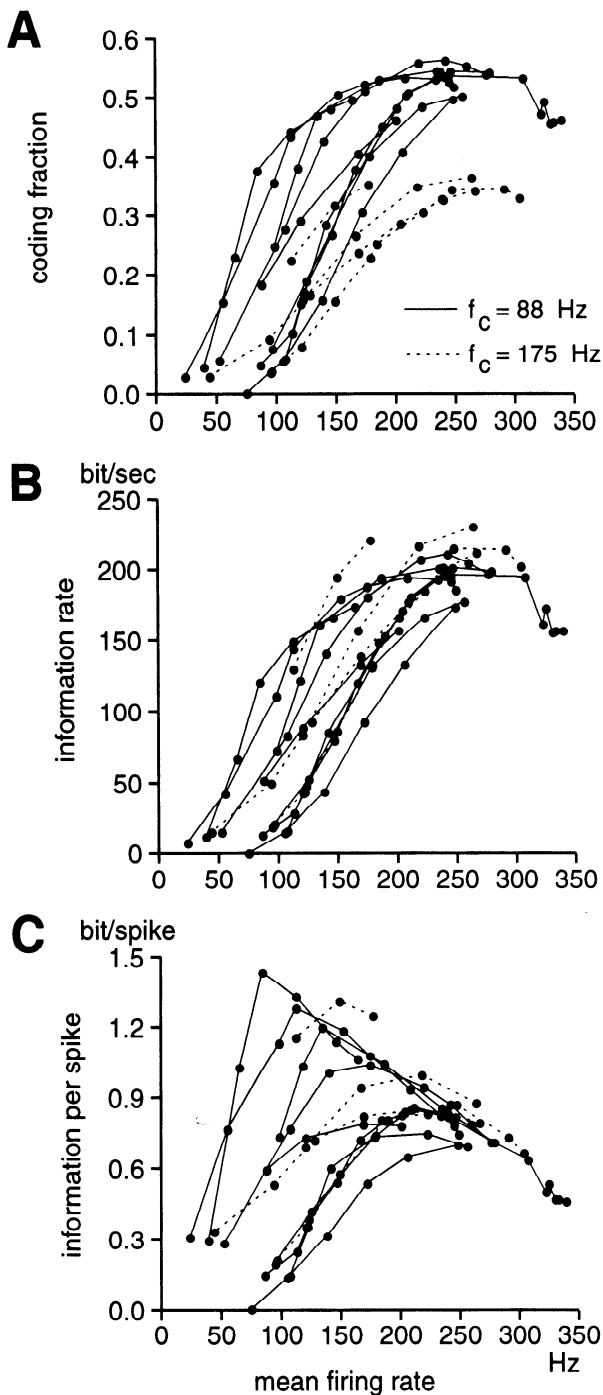


FIG. 6. A: coding fraction as a function of mean firing rate for 13 units studied at 2 different  $f_c$ s, 88 Hz (—, 9 units) and 175 Hz (---, 4 units). B and C: rates of mutual information transmission and mutual information transmitted per spike, respectively, for the same 13 units.

larger mean firing rates the initial slope was larger and saturation was reached at a lower value of the standard deviation. This suggested that the variability observed might be caused by different mean firing rates between experiments. To substantiate this hypothesis, we took each experiment, averaged the coding fraction for all values of the standard deviation used, and plotted it against the mean firing rate (which was fairly constant, see Fig. 7A2) minus the spontaneous activity.

This plot is shown in the *inset* of Fig. 8A. There is a good correlation between mean coding fraction and mean minus spontaneous firing rate (Kendall's  $\tau$  statistics and D statistics,  $\alpha < 0.01$ ) (Lehmann 1975), thus confirming that different mean minus spontaneous firing rates account for the observed variation between experiments.

#### DISCUSSION

We quantified the encoding of information in P-type electroreceptor afferents of the electric fish, *Eigenmannia*, by reconstructing part of the stimuli from the recorded spike trains. This can be thought of as characterizing the temporal aspects of the afferents receptive field by the use of engineering criteria. Specifically, we characterized coding performance by the signal-to-noise ratio, the mutual information rate, and, for the first time in this context, by the coding fraction, an absolute measure of the fraction of the stimulus that has been coded in the spike trains. Using this model system, we explored the more general question of how the coding performance depends on the statistics of the stimulus and the spontaneous and driven activity of a single neuron. We find that, despite the noisy nature of these spike trains and their high spontaneous discharge rate, single afferents can encode a significant fraction of the stimulus.

#### Technical considerations

The head-tail electric field geometry was chosen because it has been proven to be most effective in the behavioral response of the jamming avoidance response (Heiligenberg et al. 1978) and thus may be expected to be the closest approximation to the natural field geometry. However, it has the disadvantage of being inhomogeneous. The strongest distinction between T- and P-type electroreceptor afferents is the threshold amplitude for 1:1 phase-locking. Because the exact location of the receptors was not mapped in these experiments and the electric field was inhomogeneous, this distinction is subject to a degree of uncertainty. Thus some of the units selected to be P-type afferents might be understimulated T-type afferents. However, in our data analysis (see RESULTS) we did not find any hints that might justify two distinct types of afferents. This suggests that, most probably, all units selected were P-type afferents or, alternatively, that P- and T-type afferents described in previous studies cannot be distinguished by their physiological response in this analysis because the amplitude of the electric field was adjusted differently from previous studies. That the physiological differences in electroreceptor afferent types is an amplitude-dependent phenomenon was suggested earlier (Bastian and Heiligenberg 1980; Viancour 1979).

#### Reverse correlation and linear reconstruction filter

The reverse correlation of the amplitude modulation with the spike train (see Fig. 2D) shows that spikes were typically triggered by a large positive slope in the stimulus. Similar observations have been made for spike generation in retinal ganglion cells with optical stimuli (Warland and Meister 1993) and for spike generation by white noise current injection in neocortical neurons as well as in other preparations (see Mainen and Sejnowski 1995, as well as the references given

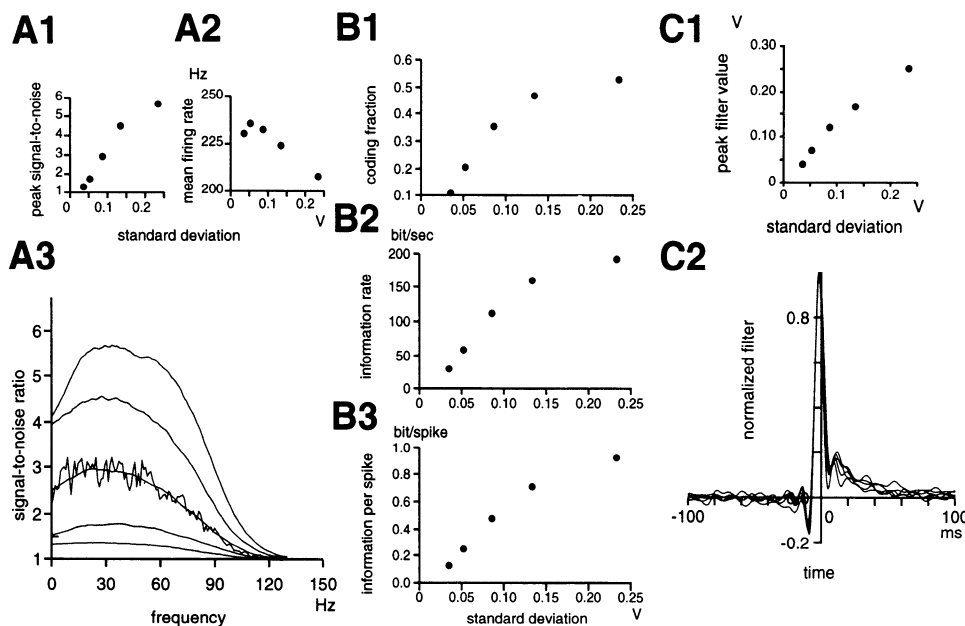


FIG. 7. Influence of standard deviation on coding for 1 unit. In the visual domain, this would correspond to the Weber contrast. A3: signal-to-noise ratio increases with increasing standard deviation ( $\sigma = 0.03, 0.05, 0.09, 0.13, \text{ and } 0.23 \text{ V}$ ); the signal-to-noise ratio has been smoothed as in Fig. 5A). A1: peak signal-to-noise ratio as a function of standard deviation. A2: mean firing rate as a function of standard deviation. B1–B3: coding fraction, rate of mutual information transmission and mutual information transmitted per spike as a function of standard deviation. C2: typical normalized filters obtained for the same unit at the same values of the standard deviation. C1: peak filter value as a function of standard deviation.

there). In the limit of low firing rate, the optimal linear reconstruction filter,  $h(t)$ , was shown to be the reverse correlation divided by the mean firing rate in idealized model neurons that linearly filter and half-wave rectify a time-varying stimulus and then encode it through changes in their instantaneous firing rate (Gabbiani and Koch 1996). Thus one can expect the reconstructions based on these two functions to have identical coding fractions in the limit of low firing rates. This theoretical prediction is in agreement with the present experimental results (see Fig. 5B1). Although neither the biophysical interpretation nor the computational properties that could be read from the reconstruction filter are obvious (see for example Gabbiani and Koch 1996; Poggio 1978), the filter  $h(t)$  is an important component of the present analysis. Our results show that  $h(t)$  changes when the statistics of the stimulus ( $f_c$ ) or the mean firing rate of the unit changes, as well as across units (see Figs. 3, B3 and C3, 4B3, and 5C2). These observations are in agreement with theoretical predictions (Gabbiani and Koch 1996) and argue against the notion—expressed previously (see, for instance, Bialek et al. 1991)—that single cells might explicitly reconstruct the stimuli at the level of single synapses from presynaptic spike trains. Such reconstructions would require substantial changes of the postsynaptic voltage waveform [corresponding to the observed changes in  $h(t)$ ] in response to changes in stimulus parameters or changes in biophysical parameters of the presynaptic cell, such as the mean firing rate. A further practical implication of these observations is that the present stochastic estimation method is powerful in quantifying the coding of white noise stimuli with stationary statistics, but more elaborated techniques will have to be used to study the coding of stimuli with nonstationary statistics, or if the spike train is not stationary in response to the stimulus.

### The existence of nonlinearities

In a linear system, the signal-to-noise ratio at a given frequency  $f_0$  (see Eq. 6) will be independent of other frequency components of the stimulus (Gabbiani 1996; Gabbiani and Koch 1996). The present experiments show that adding high frequencies to the stimulus reduced the signal-to-noise ratio at low frequencies (see Fig. 4C). This indicates a nonlinearity of the receptors' response to electric field amplitude modulations. The observed nonlinearity was small when compared with changes in signal-to-noise ratio obtained by raising the mean firing rate (Fig. 5A) or the power spectral density of the stimulus (Fig. 7, A1 and A3). These two latter effects are consistent with simplified linear models, except near saturation (see Figs. 5A1 and 7A1) (Gabbiani 1996; Gabbiani and Koch 1996). A Wiener kernel analysis and modeling of electric field amplitude coding in electroreceptor afferents (Xu et al. 1994) may allow for a more detailed study of these observations.

### Temporal bandwidth, sampling theorem, and natural stimuli

According to the sampling theorem, a system with sampling frequency  $f_s$  has a maximal temporal bandwidth  $f_s/2$ . Because electroreceptor afferents fire maximally one spike per carrier cycle and thus sample the amplitude of the electric field maximally at  $f_{\text{carrier}}$  (which was typically slightly larger than 400 Hz), one expects no encoding of stimulus frequencies  $>200 \text{ Hz}$ . From the calculated signal-to-noise ratio we read an effective temporal bandwidth of typically 200 Hz for wide-band white noise stimuli (see Fig. 3A1). This is half the sampling frequency of the units, and our results

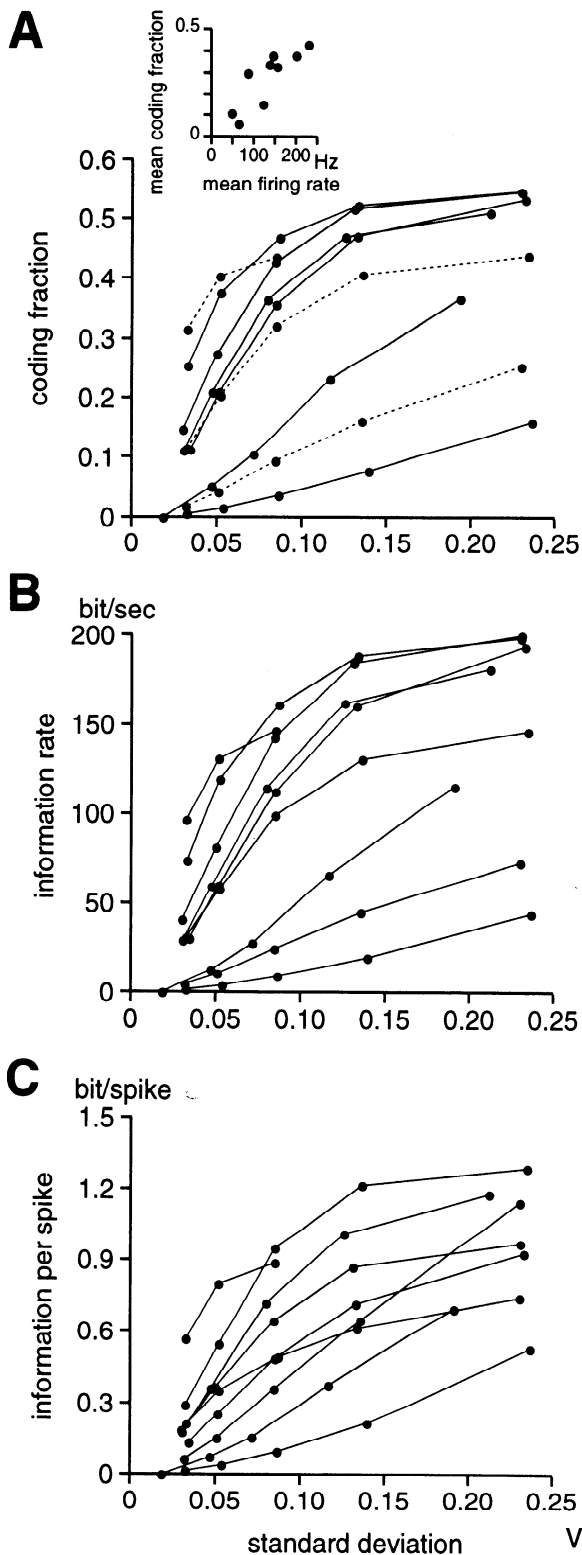


FIG. 8. A: coding fraction vs. standard deviation for 9 experiments performed at the same  $f_c$ . The 3 experiments connected by dashed lines were all performed on the same unit, but at 3 different mean firing rates ( $\lambda = 70, 110, \text{ and } 170 \text{ Hz}$  from the lowest to the highest coding fraction, respectively; this corresponds to 3 different values of  $A_o$ ;  $A_{sf} = 0.2, 0.4, \text{ and } 0.6 \text{ mV/cm}$ ). Inset: mean coding fraction is plotted against the mean firing rate minus the spontaneous activity (the averages are taken over all the standard deviations tested) for the 9 experiments. This shows a good correlation between the 2 variables. B and C: rate of mutual information transmission and mutual information per spike for the same experiments.

are thus consistent with the limits imposed by the sampling theorem. So far, the typical power spectrum of natural amplitude modulations around the fish in its natural habitat has not been measured. However, amplitude modulations caused by small moving objects have been estimated to be between 2 and 80 Hz (on the basis of typical velocity of the fish, Bastian 1981). As illustrated in Figs. 3 and 4A, the signal-to-noise ratio and the fraction of the signal encoded in single spike trains increased as the cutoff frequency of the stimulus was decreased between 740 and 88 Hz. In subsequent experiments, we verified that these results hold for  $f_c$ s down to 2 Hz ( $N = 3$  units tested at  $f_c = 2, 20, \text{ and } 50 \text{ Hz}$ ,  $\gamma$  increased up to 0.67 and the peak signal-to-noise ratio up to 12:1 for the lowest  $f_c, 2 \text{ Hz}$ ).

#### Mean firing rate, dynamic range and spontaneous activity

The mean firing rate,  $\lambda$ , increases with the mean amplitude,  $A_o$  (or equivalently with  $A_{sf}$ ), of the electric field. Thus we were able to study the coding performance as a function of the mean firing rate by changing the mean amplitude of the stimulus. Because  $A(t) = A_o + A_o s(t)$ , changing  $A_o$  also changes the absolute standard deviation of  $A_o s(t)$  while the contrast,  $\sigma$ , of the stimulus is kept constant [the standard deviation of  $s(t)$ , also known as Weber contrast in visual psychophysics].

The signal-to-noise ratio, the mutual information rate, and the coding fraction increased with increasing mean firing rate (and fixed contrast) within the dynamic range of the unit (i.e., for firing rates between the spontaneous activity and half of  $f_{carrier}$ ; see Figs. 5 and 6). Coding started for mean firing rates 20–40 Hz above the spontaneous discharge and both coding fraction and mutual information rate reached a maximum at about half of  $f_{carrier}$ . Furthermore, we found a differential sensitivity of the coding fraction and the rate of mutual information transmission as  $f_c$  of the stimulus was changed (see Fig. 6, A and B). Although the coding fraction increased more slowly with mean firing rate at higher  $f_c$ s, the increase in mutual information transmitted with mean firing rate remained largely unchanged. This indicates that the decreased gain in coding fraction was compensated by the increased  $f_c$  when the rate of mutual information transmission was computed (see Eq. 7). That the rate of mutual information transmission and coding fraction might show a differential gain sensitivity as a function of  $f_c$  was suggested by theoretical work (Gabbiani and Koch 1996). The mutual information transmitted per spike increased with mean firing rate and peaked close to saturation of the coding fraction (Fig. 6C). This behavior is different from the one predicted in simple neuronal models (Gabbiani and Koch 1996) but can easily be explained by the absence of spontaneous activity in these models.

The mean firing rate of amplitude coding electroreceptor afferents in the uncurarized but anesthetized fish, i.e., with the natural electric field established by the electric organ, has been measured to be between 30 and 75 Hz for fish with an  $f_{carrier}$  of  $\sim 300 \text{ Hz}$  (Scheich et al. 1973). The anesthetic used in these experiments (tricaine methanesulphonate) is known to reduce the spontaneous activity and the EOD frequency (Hopkins 1976) and thus the mean firing rate in an untreated fish may be higher than the one measured by

Scheich et al. (1973). Although the mean firing rate in an untreated fish is difficult to measure, the evidence cited above suggests that the natural mean firing rate may be below the range of optimal performance.

#### Standard deviation or contrast

The coding fraction, as well as the mutual information rate, increased with increasing standard deviation of the white noise,  $s(t)$ , within the dynamic range of the afferents (see Figs. 7 and 8). Because the mean firing rate was usually constant when the standard deviation was changed (Fig. 7A2), improved performance at high contrasts was not due to an increase in mean firing rate. For very high firing frequencies ( $>265$  Hz, near saturation) an increase in contrast caused a decrease in mean firing rate (as is expected, because the stimulus voltage spends less time at values causing the unit firing rate to saturate). This still resulted in improved reconstructions. The coding fraction was expected to peak and then decrease with increasing standard deviation. The latter decrease was not observed in the present experiments, most probably because very high ( $>0.25$  V) standard deviations could not be generated under our experimental conditions (see METHODS).

#### Upper bound on the performance of P receptors

Because P-type electroreceptor afferents fire either no or a single spike per carrier cycle, an upper bound for the mutual information about the amplitude modulation conveyed by a single spike train is given (in bits per s) by  $f_{\text{carrier}}$  (in Hz; Hagiwara and Morita 1963). Thus the P receptor units studied here cannot convey  $>400$  bits per second of mutual information about the stimulus. Setting  $I_{\epsilon} = f_{\text{carrier}}$  in Eq. 7 for the  $\epsilon$ -entropy leads to an upper bound for the fraction of the signal that can be theoretically encoded if the stimulus is Gaussian

$$\gamma_{\text{ub}} = 1 - \exp\left[-\frac{f_{\text{carrier}}}{2f_c} \log(2)\right] \quad (8)$$

This upper bound increases with the ratio  $f_{\text{carrier}}/f_c$  and for  $f_{\text{carrier}} = 400$  Hz,  $f_c = 100$  Hz, as was typically used in these experiments, we find  $\gamma_{\text{ub}} = 0.75$ . Thus individual P receptors encode more than half of the information that can in principle be encoded about the stimulus (see Figs. 6A and 8A and compare  $\gamma$  with  $\gamma_{\text{ub}}$  in Table 1).

#### Implications for information processing—behavioral relevance

The electric sense is used by weakly electric fish to locate objects as well as for social communication. In both cases, electric field amplitude modulations are a necessary component of the sensory stimulus used by the fish. It is thus of importance to characterize the fidelity with which single P receptor afferents are able to pass amplitude information on to the CNS. This was performed in this study by assessing the portion of amplitude modulations that could be reconstructed from single spike trains of P-type afferents. The parameters tested include a wide range of mean firing frequencies (mean electric field amplitudes), contrast values

and  $f_c$ s expected to be relevant for electrolocation (Bastian 1981) and, presumably, for electrocommunication.

In this context, our two main results are as follows. 1) The information transmitted by P receptors depends on the mean firing rate of the afferents, the  $f_c$  of the stimulus and its contrast. This provides, to the best of our knowledge, the first experimental evidence that such stimulus and biophysical parameters can influence the accuracy of information transmission in single spike trains. We expect that similar results will hold at early stages in the pathway of the mammalian visual system as well. 2) Individual P receptors are able to convey an accurate (up to 67%) and efficient ( $>1/2$  of the theoretical maximum) representation of electric stimuli on to the next processing station of the amplitude pathway, the electrosensory lateral line lobe. The coding accuracy of individual neurons could be improved at this stage by averaging over receptor afferents (the convergence of afferents onto basilar pyramidal cells, for example, has been estimated to range between 6 and 20) (Shumway 1989). Although it is unclear at present how such information is used for electrolocation, behaviorally it is known that *Eigenmannia* is able to sense extremely small changes in electric field amplitude modulations (at least down to the 1% level) (Kawasaki et al. 1988; Rose and Heiligenberg 1985). In this context, it would be particularly interesting to correlate the quantitative measures of coding, such as the signal-to-noise ratio, the coding fraction, and the mutual information rate with a measure of behavioral performance. It presently appears difficult to design a behavioral paradigm answering these questions. However, the power of the method used here also relies on the fact that the reconstructions and the measures of coding may be compared quantitatively at different stages of an information processing pathway. Convergence of sensory information may lead to an increase of the coding fraction (see above). Conversely, if the coding fraction decreases, the reconstructions could reveal which features of the stimulus were extracted between two stages of a sensory pathway.

We are indebted to the late W. Heiligenberg and to J. Spiro and C. Wong for technical assistance. The authors also thank W. Metzner for a critical reading of the manuscript.

This work was supported by a grant from the National Institutes of Health to W. Heiligenberg, by a grant from the National Science Foundation, by the Center for Neuromorphic Systems Engineering as a part of the National Science Foundation Engineering Research Center Program, and by the California Trade and Commerce Agency, Office of Strategic Technology.

Address for reprint requests: R. Wessel, Dept. of Biology, UCSD, Gilman Dr., La Jolla, CA 92093-0357.

Received 21 September 1995; accepted in final form 27 December 1995.

#### REFERENCES

- BASTIAN, J. Electrolocation. 1. How the electroreceptors of *Apteronotus albifrons* code for moving objects and other electrical stimuli. *J. Comp. Physiol.* 144: 465–479, 1981.
- BASTIAN, J. Electrolocation. In: *Electroreception*, edited by T. H. Bullock and W. Heiligenberg. New York: Wiley, 1986, p. 577–611.
- BASTIAN, J. AND HEILIGENBERG, W. Neural correlates of the jamming avoidance response of *Eigenmannia*. *J. Comp. Physiol.* 136: 135–152, 1980.
- BIALEK, W., DE RUYTER VAN STEVENINCK, R., AND WARLAND, D. Reading a neural code. *Science Wash. DC* 252: 1854–1857, 1991.
- BRONSHTEIN, I. N. AND SEMENDYAYEV, K. A. *Handbook of Mathematics*. New York: Van Nostrand Reinhold, 1985.

- BULLOCK, T. H. AND HEILIGENBERG, W. *Electroreception*. New York: Wiley, 1986.
- DE BOER, E. AND KUYPER, P. Triggered correlation. *IEEE Trans. Biomed. Eng.* 15: 169–179, 1968.
- FRANKLIN, J. AND BAIR, W. The effect of a refractory period on the power spectrum of neuronal discharges. *SIAM J. Appl. Math.* 55: 1074–1093, 1995.
- GABBIANI, F. Coding of time-varying signals in spike trains of linear and half-wave rectifying neurons. *Network Comp. Neural Syst.* 7: 61–85, 1996.
- GABBIANI, F. AND KOCH, C. Coding of time-varying signals in spike trains of integrate-and-fire neurons. *Neural Comput.* 8: 44–66, 1996.
- GIELEN, C., HESSELMANS, G., AND JOHANNESMA, P. Sensory interpretation of neural activity patterns. *Math. Biosci.* 88: 15–35, 1988.
- HAGIWARA, S. AND MORITA, H. Coding mechanisms of electroreceptor fibers in some electric fish. *J. Neurophysiol.* 26: 551–567, 1963.
- HEIDEN, C. Power spectrum of stochastic pulse sequences with correlation between the pulse parameters. *Phys. Rev.* 188: 319–326, 1969.
- HEILIGENBERG, W. Jamming avoidance responses. Model systems for neuroethology. In: *Electroreception*, edited by T. H. Bullock, and W. Heiligenberg. New York: Wiley, 1986, p. 613–649.
- HEILIGENBERG, W. *Neural Nets in Electric Fish*. Cambridge, MA: MIT Press, 1991.
- HEILIGENBERG, W., BAKER, C., AND MATSUBARA, J. The jamming avoidance response in *Eigenmannia* revisited: the structure of a neuronal democracy. *J. Comp. Physiol.* 127: 267–286, 1978.
- HEILIGENBERG, W. AND PARTRIDGE, B. L. How electroreceptors encode JAR-eliciting stimulus regimes: reading trajectories in a phase-amplitude plane. *J. Comp. Physiol.* 142: 295–308, 1981.
- HOPKINS, C. D. Stimulus filtering and electroreception: tuberous electroreceptors in three species of gymnotoid fish. *J. Comp. Physiol.* 111: 171–207, 1976.
- KAWASAKI, M., ROSE, G., AND HEILIGENBERG, W. Temporal hyperacuity in single neurons of electric fish. *Nature Lond.* 336: 173–176, 1988.
- KOLMOGOROV, A. N. On the Shannon theory of information transmission in the case of continuous signals. *IRE Trans. Inform. Theory* 2: 102–108, 1956.
- LEHMANN, E. *Nonparametrics, Statistical Methods Based on Ranks*. New York: McGraw-Hill, 1975.
- LUKES, T. Sequences of stochastic pulses. *Proc. Phys. Soc. Lond.* 78: 153–168, 1961.
- MAINEN, Z. F. AND SEJNOWSKI, T. J. Reliability of spike timing in neocortical neurons. *Science Wash. DC* 268: 1503–1506, 1995.
- MILTON, J. S. AND ARNOLD, J. C. *Introduction to Probability and Statistics* (3rd ed.). New York: McGraw-Hill, 1995.
- OPPENHEIM, A. V. AND SCHAFER, R. *Discrete-Time Signal Processing*. London: Prentice-Hall, 1989.
- POGGIO, T. Wiener-like identification techniques. In: *Theoretical Approaches in Neurobiology*, edited by W. E. Reichardt and T. Poggio. Cambridge, MA: MIT Press, 1978, p. 60–63.
- POOR, H. V. *An Introduction to Signal Detection and Estimation*. Berlin: Springer-Verlag, 1994.
- PRESS, W. H., TEUKOLSKY, S. A., VETTERLING, W., AND FLANNERY, B. *Numerical Recipes in C* (2nd ed.). Cambridge, UK: Cambridge Univ. Press, 1992.
- RIEKE, F., WARLAND, D., AND BIALEK, W. Coding efficiency and information rates in sensory neurons. *Europhys. Lett.* 22: 151–156, 1993.
- ROSE, G. AND HEILIGENBERG, W. Temporal hyperacuity in the electric sense of fish. *Nature Lond.* 318: 178–180, 1985.
- SALEH, B. *Photoelectron Statistics*. Berlin: Springer-Verlag, 1978.
- SANCHEZ, D. Y. AND ZAKON, H. H. The effects of postembryonic receptor cell addition on the response properties of electroreceptive afferents. *J. Neurosci.* 10: 361–369, 1990.
- SCHIECH, H., BULLOCK, T. H., AND HAMSTRA, R. H. Coding properties of two classes of afferent nerve fibers: high frequency electroreceptors in the electric fish, *Eigenmannia*. *J. Neurophysiol.* 36: 39–60, 1973.
- SHANNON, C. E. The mathematical theory of communication. In: *The Mathematical Theory of Communication*, edited by C. E. Shannon and W. Weaver. Urbana, IL: Illinois Univ. Press, 1963, p. 31–125.
- SHUMWAY, C. A. Multiple electrosensory maps in the medulla of weakly gymnotiform fish. II. Anatomical differences. *J. Neurosci.* 9: 4400–4415, 1989.
- THEUNISSEN, F., RODDEY, C., STUFFLEBEAM, S., CLAGUE, H., AND MILLER, J. Information theoretic analysis of dynamical encoding in the cricket cercal system. I. Four primary sensory interneurons. *J. Neurophysiol.* 75: 1345–1364, 1996.
- VIANCOUR, T. A. Electroreceptors of weakly electric fish. *J. Comp. Physiol.* 133: 317–325, 1979.
- WARLAND, D. K. AND MEISTER, M. The decoding of multi-neuronal signals from the retina. *Soc. Neurosci. Abstr.* 519: 12, 1993.
- WIENER, N. *Extrapolation, Interpolation, and Smoothing of Stationary Time Series*. New York: Wiley, 1949.
- XU, Z., PAYNE, J. R., AND NELSON, M. E. System identification and modeling of primary electrosensory afferent response dynamics. In: *Computation in Neurons and Neuronal Systems*, edited by F. H. Eeckman. Boston, MA: Kluwer, 1994, p. 197–202.
- ZAKON, H. H. The electroreceptive periphery. In: *Electroreception*, edited by T. H. Bullock and W. Heiligenberg. New York: Wiley, 1986, p. 103–156.
- ZAKON, H. H. Variation in the mode of receptor cell addition in the electrosensory system of gymnotiform fish. *J. Comp. Neurol.* 262: 195–214, 1987.